

Penicillin-binding protein 1A mutation-positive *Helicobacter pylori* promotes epithelial-mesenchymal transition in gastric cancer via the suppression of microRNA-134

LU HUANG^{1*}, ZHI-YONG WANG^{2*} and DAO-DONG PAN^{1,3}

¹College of Life Science, Nanjing Normal University, Nanjing, Jiangsu 210023;

²Department of Surgical Oncology, Jiangsu Province Hospital of TCM, Affiliated Hospital of Nanjing University of TCM, Nanjing, Jiangsu 214504; ³School of Marine Science, Ningbo University, Ningbo, Zhejiang 315211, P.R. China

Received June 11, 2018; Accepted August 24, 2018

DOI: 10.3892/ijo.2018.4665

Abstract. Evidence suggests that *Helicobacter pylori* (*H. pylori*) is not only the main cause of gastric cancer (GC), but is also closely associated with its metastasis. One of the major virulence factors in *H. pylori* is the cytotoxin-associated gene A (CagA). With the growing proportion of amoxicillin-resistant *H. pylori* strains, the present study aimed to explore the effects of CagA- and penicillin-binding protein 1A (PBP1A) mutation-positive *H. pylori* (*H. pylori*_{CagA+/P+}) on GC cells, and its clinical significance. The clinical significance of *H. pylori*_{CagA+/P+} infection was analyzed in patients with GC. *In vitro*, GC cells were infected with *H. pylori*_{CagA+/P+} to investigate whether it was involved in the epithelial-mesenchymal transition (EMT) of SGC-7901 cells using immunofluorescence and western blot analysis. The results of clinical analysis demonstrated that, although CagA-negative *H. pylori* infection had no significant association with the characteristics of patients with GC, *H. pylori*_{CagA+/P+} infection was significantly associated with various clinicopathological parameters, including invasion depth, lymphatic metastasis and distant metastasis. *In vitro*, the results indicated that *H. pylori*_{CagA+/P+} promoted proliferation, invasion and EMT of SGC-7901 cells. MicroRNA (miR)-134 was downregulated in *H. pylori*_{CagA+/P+} infected tissues compared with those with *H. pylori*_{CagA+/P-}

infection. miR-134 overexpression significantly reversed *H. pylori*_{CagA+/P+} infection-associated cell proliferation, invasion and EMT. Furthermore, the results revealed that Forkhead box protein M1 (FoxM1) was a direct target of miR-134, and FoxM1 knockdown impeded *H. pylori*_{CagA+/P+}-induced EMT. In conclusion, the present study demonstrated that miR-134 may suppress the proliferation, invasion and EMT of SGC-7901 cells by targeting FoxM1, and may serve a protective role in the process of *H. pylori*_{CagA+/P+}-induced GC. These findings may lead to an improved understanding of *H. pylori*_{CagA+/P+}-associated poor clinical characteristics in patients with GC.

Introduction

Helicobacter pylori (*H. pylori*) is a gram-negative, microaerophilic bacterium that colonizes the gastric mucosa and infects ~50% of individuals worldwide. It has been categorized as a group I carcinogen for gastric cancer (GC) by the World Health Organization, and GC remains a major public health problem worldwide (1,2). A previous study revealed that the relative risk for the development of GC was 3.8-fold higher in patients with *H. pylori* infection compared to those without (3). In addition, the association between *H. pylori* eradication and the reduced incidence of GC has been demonstrated in a meta-analysis study (4). Nevertheless, with regards to the prognosis of GC, several studies have suggested that *H. pylori* infection is a favorable prognostic factor of GC in a Chinese prospective cohort (5,6). Conversely, other studies have indicated that *H. pylori* infection has no association with prognosis in Chinese patients (7,8). It was hypothesized that this discrepancy may be due to the fact that GC with different *H. pylori* genotypes exhibits different growth patterns and pathobiological behavior, indicating different mechanisms of cancer progression. Further knowledge regarding *H. pylori*-infected GC may help to identify novel therapeutic targets.

Treatment of *H. pylori* infection is often empiric and current guidelines recommend against the use of standard triple therapy (clarithromycin, amoxicillin and proton pump inhibitors) as first-line treatment (9). However, the prevalence of amoxicillin-resistant *H. pylori* is very high in Africa (65.6%) and Asia (11.6%) (9,10). In *H. pylori*, resistance occurs through

Correspondence to: Dr Dao-Dong Pan, College of Life Science, Nanjing Normal University, 1 Wenyuan Road, Nanjing, Jiangsu 210023, P.R. China
E-mail: daodongp009@163.com

*Contributed equally

Abbreviations: *H. pylori*, *Helicobacter pylori*; GC, gastric cancer; CagA, cytotoxin-associated gene A; PBP1A, penicillin-binding protein 1A; FoxM1, Forkhead box M1; miRNAs/miRs, microRNAs; EMT, epithelial-mesenchymal transition

Key words: gastric cancer, *Helicobacter pylori*, penicillin-binding protein 1A, microRNAs, epithelial-mesenchymal transition

modifications in penicillin-binding proteins (PBPs), leading to a decreased affinity for the drug. These modifications include mutations and/or mosaics in PBP2X and PBP2B, as well as in PBP1A for the highly resistant isolates (11). To date, the clinical significance of amoxicillin-resistant *H. pylori* (PBP1A mutation-positive *H. pylori*, *H. pylori*_{P+}) in GC, and the role of *H. pylori*_{P+} in GC cell malignant behavior and its specific mechanism require further elucidation. Furthermore, the *H. pylori* genome shows genetic diversity among distinct isolates, and *H. pylori* pathogenicity is different in distinct isolates. Clinically isolated *H. pylori* strains are often subdivided into two types according to the cytotoxin-associated gene (Cag) pathogenicity island-encoded CagA protein (12). Notably, CagA-positive *H. pylori* increases the risk for GC over the risk associated with *H. pylori* infection alone (13). In addition, it has been reported that infections involving *H. pylori* strains that possess the virulence factor CagA have a worse clinical outcome than those involving CagA-negative strains (14), and CagA is indispensable for *H. pylori*-induced tumorigenesis in GC (15). Furthermore, CagA may promote epithelial-mesenchymal transition (EMT), which indicates a strong ability to induce invasion and metastasis of tumor cells, and to stimulate gastric carcinogenesis (16). Therefore, in the present study, the role of CagA- and PBP1A mutation-positive *H. pylori* (*H. pylori*_{CagA+/P+}) was investigated in patients with GC and in GC cells, in order to gain insights into the effects of *H. pylori* during the development of GC.

Factors intrinsic to the host may also contribute to the emergence of GC, and microRNAs (miRNAs/miRs) appear to serve an important role in the etiology of this disease (17). miRNAs are noncoding RNAs that are involved in post-translational regulation of gene expression (18). Unique miRNAs are associated with various histological subtypes, and the progression and prognosis of GC (19). A previous study demonstrated that *H. pylori* may induce dysregulation of miRNAs, contributing to the etiology of *H. pylori*-mediated GC cases (17). Therefore, the identification of signature miRNAs associated with *H. pylori* infection may provide novel insights into its carcinogenesis and the host mechanisms that are involved in bacterial elimination. However, whether miRNAs are involved in the effects of *H. pylori*_{CagA+/P+} on GC has received little attention.

The present study investigated the clinical significance of *H. pylori*_{CagA+/P+} in patients with GC, and explored the role of *H. pylori*_{CagA+/P+} in cell proliferation, invasion and EMT of GC cells *in vitro*, in order to uncover the potential mechanism underlying the effects of *H. pylori*_{CagA+/P+} on gastric carcinogenesis. Furthermore, the involvement of potential miRNAs in the pathogenesis of *H. pylori*_{CagA+/P+}-associated GC was observed.

Materials and methods

Patients, *H. pylori* strains and culture conditions. The present study was conducted between February 2014 and November 2017 at the Jiangsu Province Hospital of TCM (Nanjing, China). Gastric biopsy specimens were collected and maintained in selective tryptic soy broth as transport media for further processing, as recommended by Siu *et al* (20). Only patients who were diagnosed with GC, and were negative or positive for *H. pylori* were recruited; patient characteristics are presented

in Table I. A total of 184 pairs of GC tissues and adjacent non-tumor tissues were collected during surgery. None of the patients had received adjuvant chemotherapy, radiotherapy or *H. pylori* eradication treatment prior to surgery. The histological types, stages and types of treatment of the patients with GC were recorded. Samples obtained from each patient were collected for culture, and three clinical isolates were recovered from GC tissues, as previously described (21), which were used in the present study. Identification of *H. pylori* was determined by colony morphology, Gram-staining, and biochemical profile reactions, such as oxidase, catalase and urease tests (22). The molecular identification of CagA-positive and CagA-negative strains was conducted as previously described (23). The amoxicillin-susceptible and amoxicillin-resistant *H. pylori* strains examined in this study were isolated from GC tissues. Amoxicillin resistance was identified by sub-culturing swabs of bacteria from isolation plates to horse blood agar plates with and without 0.5 mg/l amoxicillin (Merck KGaA, Darmstadt, Germany), as previously described (24). A PBP1A mutation in the C-terminal region (encoded by amino acids 320-660) was validated using reverse transcription-polymerase chain reaction (RT-PCR) (22); the primers used were as follows: Forward, 5'-GCGACATCTGGATGAAAAT-3' and reverse, 5'-CCATTGTTCCAACATAATCA-3' (22). All *H. pylori* strains were cultured on chocolate blood agar, and were incubated at 37°C in a humidified incubator containing 10% CO₂ and 85% N₂ for 48 h.

Cell culture. The human gastric epithelial cell line (GES-1), and GC cell lines, MGC-803, BGC-823, SGC-7901 and MKN45, were obtained from the Cell Bank of the Chinese Academy of Sciences (Shanghai, China) and maintained in Roswell Park Memorial Institute (RPMI)-1640 medium (Sigma-Aldrich; Merck KGaA, Darmstadt, Germany) supplemented with 10% fetal bovine serum (FBS; Gibco; Thermo Fisher Scientific, Inc., Waltham, MA USA). 293T cells (Cell Bank of Chinese Academy of Sciences) were cultured in Dulbecco's modified Eagle's medium (Gibco; Thermo Fisher Scientific, Inc.) supplemented with 10% FBS. All cells were incubated at 37°C in a humidified atmosphere containing 5% CO₂.

***H. pylori* infection experiments.** For cell infection, a single colony of a 3-day old culture was cultured in 5 ml broth (tryptone 10 g/l; yeast extract 5 g/l; NaCl 10 g/l in distilled water; pH 7.4) supplemented with 10% heat-inactivated FBS (Gibco; Thermo Fisher Scientific, Inc.). The bacterial cultures were incubated under microaerobic conditions generated by CampyGen sachets at 37°C for 1-2 days with agitation at 150 rpm. When the 600 nm optical density of the bacterial culture in Brain Heart Infusion broth (HiMedia Laboratories, Mumbai, India) reached 1.0, the bacteria were harvested and incubated at 37°C in RPMI medium for 30 min. SGC-7901 cells were microscopically enumerated using an improved Neubauer counting chamber. Monolayer SGC-7901 cells in a 6-well plate (10⁵/well) were incubated with *H. pylori* at a multiplicity of infection of 50:1 for 12 h at 37°C and 10% CO₂, as previously described (25).

Cell transfection. miRNA mimic control (5'-UCACAACCUC CUAGAAAGAGUAGA-3'), miR-134 mimics (sense 5'-UGU

Table I. Association between the clinical characteristics of the study subjects and the various *H. pylori* strains.

Clinical characteristics	<i>H. pylori</i> -negative (n=50)	HP _{CagA-} (n=48)	HP _{CagA+/P-} (n=55)	HP _{CagA+/P+} (n=31)	P ^a	P ^b	P ^c
Age, years (means ± SD)	57.70±9.64	54.31±7.82	52.96±8.95	55.08±11.15	0.38	0.22	0.56
Sex							
Male	35	27	30	19	0.23	0.98	0.70
Female	15	21	25	12			
Location					0.78	0.69	0.67
Proximal	9	11	16	7			
Middle	16	16	19	10			
Distal	25	21	20	14			
Size					0.90	0.032	0.028
<5 cm	38	36	23	5			
≥5 cm	12	12	32	26			
Histological classification					0.22	0.08	0.57
Papillary adenocarcinoma	11	12	15	9			
Tubular adenocarcinoma	26	31	24	17			
Mucinous adenocarcinoma	5	1	5	2			
Signet-ring cell carcinoma	8	4	11	3			
Histological differentiation					0.19	0.25	0.14
Well	9	17	23	9			
Moderately	8	9	16	6			
Poorly	31	21	16	15			
Others	2	1	0	1			
Invasion depth					0.21	0.006	<0.0001
T1	13	20	10	4			
T2	30	19	20	2			
T3	5	5	19	9			
T4	2	4	6	16			
TNM stages					0.62	0.015	0.019
I	22	18	11	6			
II	19	23	20	4			
III	7	4	20	13			
IV	2	3	4	8			
Lymphatic metastasis					0.89	0.006	0.007
No	36	33	24	4			
Yes	14	15	31	27			
Distant metastasis					0.27	0.008	0.009
No	33	37	21	3			
Yes	17	11	34	28			

^aχ² analysis between *H. pylori*-negative and HP_{CagA-} groups; ^bχ² analysis between HP_{CagA+/P-} and HP_{CagA-} groups; ^cχ² analysis between HP_{CagA+/P-} and HP_{CagA+/P+} groups. CagA, cytotoxin-associated gene A; HP_{CagA-}, CagA-negative *H. pylori*; HP_{CagA+/P-}, CagA-positive and PBP1A mutation-negative *H. pylori*; HP_{CagA+/P+}, CagA- and PBP1A mutation-positive *H. pylori*; *H. pylori*, *Helicobacter pylori*; PBP1A, penicillin-binding protein 1A; SD, standard deviation.

GACUGGUUGACCAGAGGGG-3'; antisense 5'-CCUCUGG UCAACCAGUCACAUU-3'), inhibitor control (5'-UCACAA CCUCCUAGAAAGAGUAGA-3') and miR-134 inhibitors (5'-CCCCUCUGGUCAACCAGUCACA-3') were all purchased from Guangzhou Ribobio Co., Ltd. (Guangzhou, China). Forkhead box M1 (FoxM1)-specific small interfering RNA

(siRNA; si-FOXM1; 5'-UGAAUCUGCGUUUUC ACUCUC-3') and negative control siRNA (5'-UGCAAUAAGGGGUAUC AUGC-3') were synthesized by Shanghai GenePharma Co., Ltd. (Shanghai, China). Lipofectamine® 2000 reagent (Invitrogen; Thermo Fisher Scientific, Inc.) was used to transfect the aforementioned oligonucleotides into SGC-7901 cells according

to the manufacturer's protocol. Briefly, 5×10^5 cells were seeded into each well of 6-well plates 18–24 h prior to transfection. The transfection medium (2 ml) containing 1 $\mu\text{g}/\text{ml}$ siRNAs or 100 nmol/l miRNA mimics/inhibitors together with 6 μl Lipofectamine[®] 2000 was incubated at room temperature for 15 min and was then transferred to each well of the culture plates at 37°C; the cells were harvested for analysis after 24 h. FoxM1 overexpression was achieved by transfecting SGC-7901 cells with the FoxM1 (NM_202002) plasmid (Shanghai GeneChem Co., Ltd., Shanghai, China). Attractene transfection reagent (Qiagen GmbH, Hilden, Germany) was used to transfect cells with the FoxM1 plasmid or an empty GV230 plasmid (Shanghai GeneChem Co., Ltd.), in accordance with the manufacturer's protocol.

miRNA microarray analysis. Five CagA-positive and PBP1a mutation-negative *H. pylori* (*H. pylori*_{CagA+/IP-}) and five *H. pylori*_{CagA+/IP+} tumor tissue samples were selected for miRNA microarray analysis. Total RNA was isolated using TRIzol[®] reagent (Invitrogen; Thermo Fisher Scientific, Inc.) and miRNeasy mini kit (Qiagen GmbH), according to the manufacturers' protocols. Total RNA was then labeled using the miRCURY[™] Array Power labeling kit (Exiqon; Qiagen GmbH) and hybridization was performed using miRCURY[™] LNA Array (Exiqon; Qiagen GmbH). Fluorescent images were collected using a laser scanner (GenePix 4000B; Molecular Devices, LLC, Sunnyvale, CA, USA) and were digitized using Array-Pro image analysis software 6.3 (Media Cybernetics, Inc., Rockville, MD, USA). The SpotData Pro 3.0 software (CapitalBio Corporation, Beijing, China) was used for data analysis. Hierarchical clustering was performed using Data Matching Software MeV v4.8.1 (26).

RNA isolation and RT-quantitative (q)PCR analysis. Total RNA was extracted from the treated cells using TRIzol[®] reagent (Invitrogen; Thermo Fisher Scientific, Inc.). Total RNA was reverse transcribed using the cDNA Synthesis kit (Takara Biotechnology Co., Ltd., Dalian, China), according to the manufacturer's protocol, and quantification was performed using SYBR Green (Takara Biotechnology Co., Ltd.) on a LightCycler480 PCR system (Roche Diagnostics, Basel, Switzerland). Amplification of target gene cDNA was normalized to GAPDH expression. The expression levels of miR-134 were assessed using the Bulge-Loop[™] miRNA qRT-PCR Primer Set and the miRNA qRT-PCR Control Primer Set (Guangzhou RiboBio Co., Ltd.), and U6 was used as an internal control. The primer sequences used are listed in Table II. The thermocycling conditions were as follows: 94°C for 10 min, followed by 40 cycles at 94°C for 10 sec, 60°C for 45 sec and 72°C for 60 sec, and a final extension step at 72°C for 5 min. Each reaction was performed in triplicate. Relative quantification of gene expression levels was expressed as fold-change using the $2^{-\Delta\Delta C_q}$ method (27). Each test was carried out in triplicate.

Western blot analysis. Radioimmunoprecipitation assay lysis buffer and Bicinchoninic Acid Protein Quantification kit (Beijing Solarbio Science & Technology Co., Ltd., Beijing, China) were employed to extract total protein from SGC-7901 cells and determine protein concentration, respectively.

Equal amounts of protein (30 μg) were separated by 10–12% SDS-PAGE, transferred to polyvinylidene fluoride membranes. After blocking with 5% non-fat milk at room temperature for 1 h, the membranes were incubated with E-cadherin (cat. no. 14472, 1:1,000), Vimentin (cat. no. 5741, 1:1,000), α -smooth muscle actin (α -SMA, cat. no. 48938, 1:1,000), FoxM1 (cat. no. 20459, 1:1,000) and GAPDH (cat. no. 2118, 1:1,000; Cell Signaling Technology, Inc., Danvers, MA, USA) antibodies overnight at 4°C. The membranes were then incubated with goat anti-rabbit immunoglobulin (Ig) G H&L (horseradish peroxidase) (1:5,000; Abcam, Cambridge, MA, USA) for 1 h at room temperature. Membrane-bound immune complexes were visualized using the enhanced chemiluminescence detection reagent (Beyotime Institute of Biotechnology, Haimen, China).

Cell proliferation and invasion. Cell proliferation was measured using the Cell Counting Kit-8 (CCK-8; Dojindo Molecular Technologies, Inc., Kumamoto, Japan). At different time points, 10 μl CCK-8 solution was added to each well, and the plates were incubated at 37°C for 2 h. Absorbance was measured at 570 nm using a Thermo Fisher Scientific Microplate Reader (Thermo Fisher Scientific, Inc.). The cell invasion assay was performed using Transwell chambers coated with Matrigel (EMD Millipore, Billerica, MA, USA). At 48 h post-transfection, 10^5 cells were added into the upper chambers alongside serum-free medium. In the lower chambers, 500 μl RPMI-1640 medium containing 10% FBS was added as a chemoattractant. After 24 h, the Matrigel and cells on the upper surface were removed by cotton swabs, and the cells that had migrated to the lower surface were fixed in 4% paraformaldehyde (Sigma-Aldrich; Merck KGaA) for 15 min at room temperature and stained with 0.1% crystal violet (Sigma-Aldrich; Merck KGaA) for 15 min at room temperature. Cells were visually counted in five randomly selected fields under a light microscope (Axiovert 200 inverted microscope; Zeiss AG, Oberkochen, Germany).

Luciferase assay and constructs. TargetScan (<http://www.targetscan.org>) and microRNA database (<http://www.microrna.org>) bioinformatics software were used to predict the downstream targets of miR-134. The FoxM1 promoter region was amplified from human genomic DNA (cat. no. Roche-11691112001; Sigma-Aldrich; Merck KGaA) by PCR (forward, 5'-GGTCCGAGTAAAACAAGAGCG-3'; reverse, 5'-AGTGAGAGAGTATAGGAAGG-3'). Mutated FoxM1, devoid of the miR-134 binding site, was generated using the QuikChange II XL Site-Directed Mutagenesis kit (cat. no. ST200521; Stratagene; Agilent Technologies, Inc., Santa Clara, CA, USA). Wild type and mutated FoxM1 were sub-cloned into the pGL3-basic luciferase vector (Promega Corporation, Madison, WI, USA). 293T cells, cultured in 24-well plates (5×10^5), were transfected with 2.4 $\mu\text{g}/\text{well}$ wild type FoxM1-pGL3 plasmid or mutant FoxM1-pGL3 plasmid, and were co-transfected with 20 nmol/l miR-134 mimics or mimic control using 2 μl Lipofectamine[®] 2000 transfection reagent (Invitrogen; Thermo Fisher Scientific, Inc.), according to the manufacturer's protocol. After 48 h of transfection, luciferase activity was measured using the Bright-Glo[™] Luciferase Assay system (Promega Corporation) according to the manufacturer's protocol. Relative percentages of

Table II. Forward and reverse primers used for RT-quantitative polymerase chain reaction.

Gene name	Sequence (5'-3')
Hsa-miR-134	
RT primer	GTCGTATCCAGTGCCTGTCGTGGAGTCGGCAATTGCACTGGATACGTTGGTGTGTC
Forward	ACACTCCAGCTGGGCACCAA
Hsa-miR-218	
RT primer	GTCGTATCCAGTGCCTGTCGTGGAGTCGGCAATTGCACTGGATACGUGUAGAAA
Forward	ACACTCCAGCTGGGTTGTGCTTGATCTAA
Hsa-miR-488	
RT primer	GTCGTATCCAGTGCCTGTCGTGGAGTCGGCAATTGCACTGGATACGTTGAGAGT
Forward	ACACTCCAGCTGGGCCAGATAATGGCA
Hsa-miR-159	
RT primer	GTCGTATCCAGTGCCTGTCGTGGAGTCGGCAATTGCACTGGATACGTCCTACCC
Forward	ACACTCCAGCTGGGCAGACTTGGCCAT
U6	
Forward	CTCGCTTCGGCAGCACA
Reverse	AACGCTTCACGAATTTGCGT
E-cadherin	
Forward	AAAGGCCCATTTCTAAAAACCT
Reverse	TGCGTTCTCTATCCAGAGGCT
Vimentin	
Forward	AGTCCACTGAGTACCGGAGAC
Reverse	CATTCACGCATCTGGCGTTC
α -SMA	
Forward	CATTCACGCATCTGGCGTTC
Reverse	CCATCAGGCAGTTCGTAG
GAPDH	
Forward	TGCACCACCAACTGCTTAGC
Reverse	GGCATGGACTGTGGTCATGAG

α -SMA, α -smooth muscle actin; miR-134, microRNA-134; RT, reverse transcription.

luminescence intensity were calculated by comparison with the mimic control-transfected cells.

Immunofluorescence analysis. After treatment, cells were fixed with 4% paraformaldehyde (Sigma-Aldrich; Merck KGaA) for 15 min at room temperature and blocked with 5% bovine serum albumin (Sigma-Aldrich; Merck KGaA) for 30 min at room temperature. The cells were then incubated with E-cadherin (1:400), α -SMA (1:500) or FoxM1 (1:500) primary antibodies overnight at 4°C. After washing with PBS-0.1% Tween, cells were incubated with Alexa Fluor® 488 goat anti-rabbit IgG (cat. no. A-11034) or Alexa Fluor® 594 goat anti-rabbit IgG (cat. no. B40925; 1:500; Invitrogen; Thermo Fisher Scientific, Inc.) for 30 min at room temperature in the dark. DAPI (Sigma-Aldrich; Merck KGaA) was used to identify the nuclei. Images were captured under a Nikon Eclipse 800 epifluorescence microscope (Nikon Corporation, Tokyo, Japan) with the appropriate filters.

Statistical analysis. All experiments were performed at least three times and data are presented as the means \pm standard

error. Pearson's χ^2 test was used to investigate the associations between *H. pylori* status and categorical variables. Student's t-test was used to compare differences between two groups with continuous variables. One-way analysis of variance and least significant difference post hoc test was used to compare the differences between more than two groups. Pearson's correlation was used to analyze the relationship between miR-134 and FoxM1 expression. Statistical analyses were performed using SPSS 20.0 (IBM Corp., Armonk, NY, USA) and GraphPad Prism 6.0 (GraphPad Software Inc., La Jolla, CA, USA). $P < 0.05$ was considered to indicate a statistically significant difference.

Results

H. pylori CagA+/P+ infection is associated with poor clinicopathological characteristics in patients with GC. The study group consisted of 50 patients with *H. pylori*-negative GC, 48 patients with CagA-negative *H. pylori* (*H. pylori*_{CagA-}) GC, 55 patients with *H. pylori*_{CagA+/P-} GC, and 31 patients with *H. pylori*_{CagA+/P+} GC. As shown in Table I, the demographic and

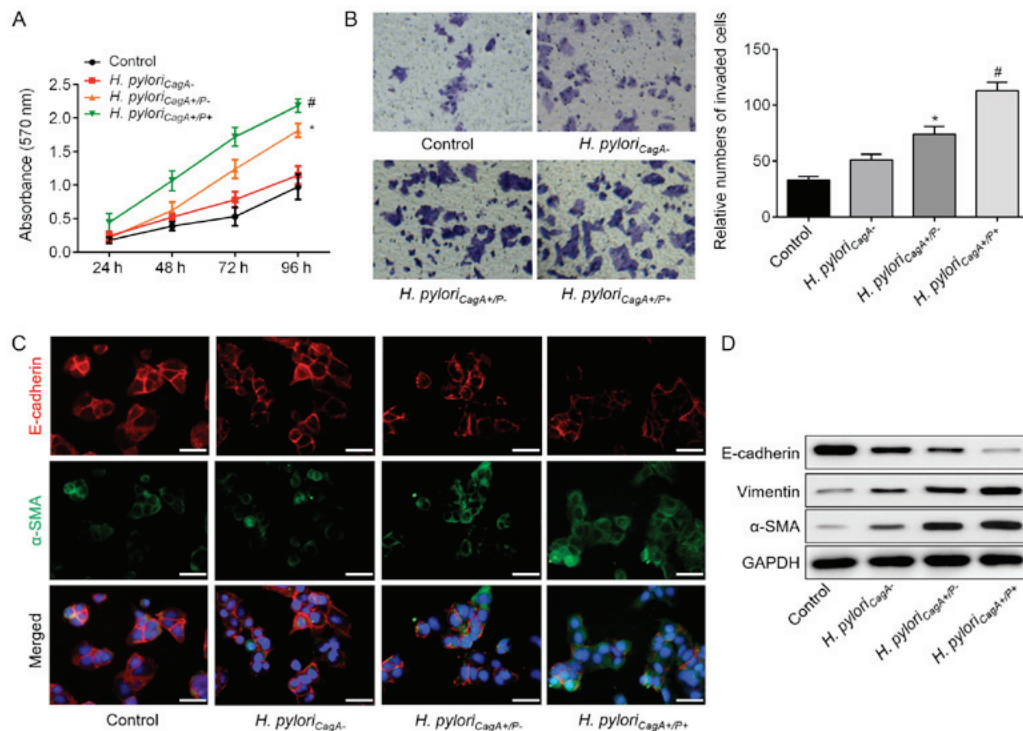


Figure 1. *H. pylori*_{CagA+/P+} induces proliferation, invasion and EMT in SGC-7901 gastric cancer cells. (A) Growth curves for SGC-7901 cells exposed to the indicated treatments via Cell Counting Kit-8 assay. (B) Transwell assay was used to evaluate the invasion of SGC-7901 cells infected with *H. pylori*_{CagA-}, *H. pylori*_{CagA+/P-} and *H. pylori*_{CagA+/P+}. Untreated SGC-7901 cells were used as a control (magnification, x100). (C) Double-labeled immunofluorescence staining was performed to examine the expression of E-cadherin (red) and α -SMA (green) in SGC-7901 cells from different groups. Images merged with DAPI are presented. Scale bar, 50 μ m. (D) Protein expression levels of E-cadherin, Vimentin and α -SMA in SGC-7901 cells infected with various *H. pylori* strains. * $P < 0.05$ vs. the control group; # $P < 0.05$ vs. the *H. pylori*_{CagA+/P-} group. α -SMA, α -smooth muscle actin; CagA, cytotoxin-associated gene A; *H. pylori*_{CagA-}, CagA-negative *H. pylori*; *H. pylori*_{CagA+/P-}, CagA-positive and PBP1A mutation-negative *H. pylori*; *H. pylori*_{CagA+/P+}, CagA- and PBP1A mutation-positive *H. pylori*; *H. pylori*, *Helicobacter pylori*; PBP1A, penicillin-binding protein 1A.

pathological characteristics of these patients were collected. There were no significant differences among the groups with regards to age, gender, tumor location, histological classification and histological differentiation. Notably, there was a statistically significant difference between *H. pylori*_{CagA+/P-} infection and *H. pylori*-negative groups with regards to tumor size, invasion depth, TNM stages, lymphatic metastasis and distant metastasis. Furthermore, patients with *H. pylori*_{CagA+/P+} exhibited poor clinicopathological characteristics compared with patients with *H. pylori*_{CagA+/P-}. These results suggested that *H. pylori*_{CagA+/P+} may have an important role in the development of GC, which differs from *H. pylori*_{CagA+/P-}.

*H. pylori*_{CagA+/P+} induces proliferation, invasion and EMT in SGC-7901 cells. The present study performed an *in vitro* assay to further investigate the mechanisms underlying the relationship between *H. pylori*_{CagA+/P+} infection and poor clinicopathological characteristics. To imitate the *in vivo* impact of different *H. pylori* strains, SGC-7901 GC cells were infected with *H. pylori*_{CagA-}, *H. pylori*_{CagA+/P-} and *H. pylori*_{CagA+/P+}. Notably, the CCK-8 assay (Fig. 1A) and Transwell assay (Fig. 1B) revealed that, when compared with the *H. pylori*_{CagA-} group, *H. pylori*_{CagA+/P-}-infected cells exhibited significantly increased cell proliferation and invasion. Furthermore, cell proliferation and invasion were further increased in *H. pylori*_{CagA+/P+}-infected GC cells, as compared to those infected with *H. pylori*_{CagA+/P-}. In addition, immunofluorescence staining revealed that *H. pylori*_{CagA+/P-} and

*H. pylori*_{CagA+/P+} infection reduced the fluorescence intensity of E-cadherin, but increased the intensity of α -SMA (Fig. 1C). Western blot analysis indicated that *H. pylori*_{CagA+/P-} infection induced EMT of SGC-7901 cells, whereas *H. pylori*_{CagA+/P+} exhibited more prominent EMT in GC cells compared with the *H. pylori*_{CagA+/P-} group (Fig. 1D). These findings may explain why patients with *H. pylori*_{CagA+/P+} and GC exhibited advanced malignant behavior compared with patients with *H. pylori*_{CagA+/P-} infection.

*miR-134 is downregulated in H. pylori*_{CagA+/P+} GC tissues and cells. To determine the potential involvement of miRNAs in gastric carcinogenesis induced by *H. pylori*_{CagA+/P-} and *H. pylori*_{CagA+/P+}, a miRNA microarray was performed on five GC tissues, which were randomly selected from the *H. pylori*_{CagA+/P-} and *H. pylori*_{CagA+/P+} groups. Notably, the results identified nine upregulated miRNAs and 11 downregulated miRNAs in the *H. pylori*_{CagA+/P+} group compared with the *H. pylori*_{CagA+/P-} group (Fig. 2A). The present study further investigated the four most downregulated miRNAs, miR-134, miR-218, miR-159 and miR-488, and validated the microarray results using RT-qPCR. The expression levels of miR-134 were decreased in the *H. pylori*_{CagA-} group compared with in the control group, and were further decreased in the *H. pylori*_{CagA+/P+} group (Fig. 2B). Although miR-218 and miR488 were decreased in *H. pylori*-infected GC tissues, there was no significant difference between the different *H. pylori* strains (Fig. 2C and D). In addition, miR-159

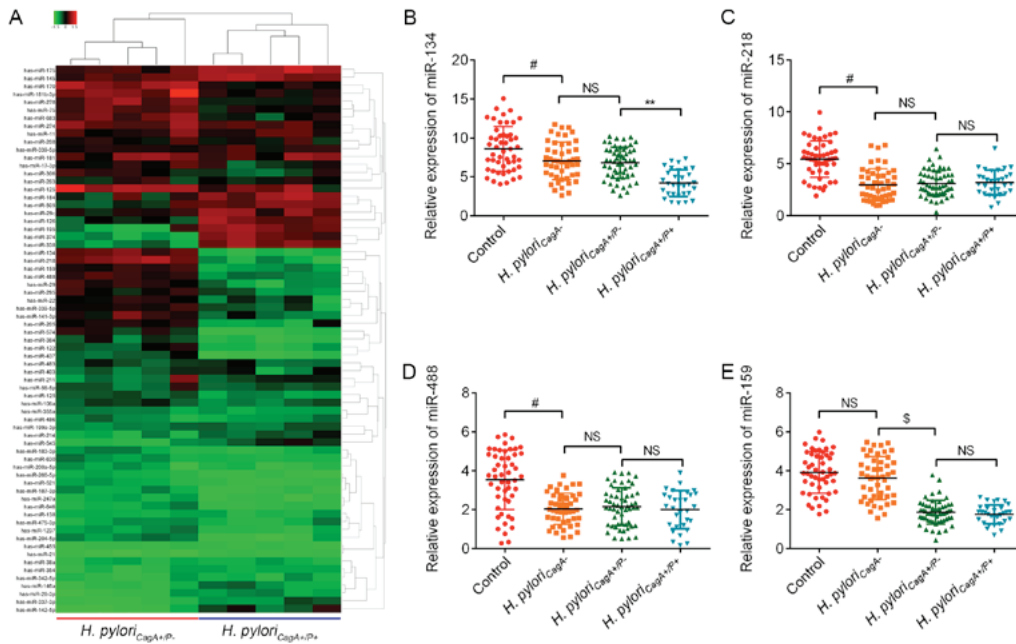


Figure 2. Aberrant miRNAs between *H. pylori*_{CagA+/P+} and *H. pylori*_{CagA+/P+} GC tissues. (A) Heatmap of miRNA expression between *H. pylori*_{CagA+/P+} and *H. pylori*_{CagA+/P+} GC tissues. The five tissues in each group were selected at random. Green, downregulated; red, upregulated. Relative expression levels of (B) miR-134, (C) miR-218, (D) miR-488 and (E) miR-159 in GC tissues without *H. pylori* infection, and in tissues infected with *H. pylori*_{CagA-}, *H. pylori*_{CagA+/P-} and *H. pylori*_{CagA+/P+}. #P < 0.05 vs. the control group; NS, not significant; **P < 0.05 vs. the *H. pylori*_{CagA+/P-} group. CagA, cytotoxin-associated gene A; *H. pylori*_{CagA-}, CagA-negative *H. pylori*; *H. pylori*_{CagA+/P-}, CagA-positive and PBP1A mutation-negative *H. pylori*; *H. pylori*_{CagA+/P+}, CagA- and PBP1A mutation-positive *H. pylori*; *H. pylori*, *Helicobacter pylori*; miR, microRNA; NS, not significant; PBP1A, penicillin-binding protein 1A.

was not altered in *H. pylori*-positive tissues compared with in *H. pylori*-negative tissues. Although miR-159 was downregulated in *H. pylori*_{CagA+/P+} and *H. pylori*_{CagA+/P+} groups, when compared with the control group, its expression did not differ between the *H. pylori*_{CagA+/P+} and *H. pylori*_{CagA+/P+} groups (Fig. 2E). Based on these findings, the present study focused on miR-134, with the aim of identifying its regulatory role in *H. pylori*_{CagA+/P+} GC tissues.

miR-134 inhibits HP-induced cell proliferation, invasion and reverses EMT. In order to elucidate the relationship between miR-134 and *H. pylori*_{CagA+/P+}-induced malignant behavior of GC cells, proliferation, invasion and EMT of SGC-7901 cells were analyzed. As shown in Fig. 3A, miR-134 expression differed between GES-1 cells and the four GC cell lines. SGC-7901 cell exhibited the lowest miR-134 expression; therefore, it was then chosen for subsequent analyses. As presented in Fig. 3B, SGC-7901 cells exposed to *H. pylori* infection exhibited reduced miR-134 expression, and cells infected with *H. pylori*_{CagA+/P+} possessed the lowest expression levels of miR-134; these findings were consistent with the results from clinical samples. Therefore, SGC-7901 cells were transfected with miR-134 mimics to induce miR-134 overexpression (Fig. 3C). Subsequently, CCK-8 and Transwell assays demonstrated that miR-134 overexpression significantly decreased *H. pylori*_{CagA+/P+}-induced cell proliferation and invasion compared with in the control group (Fig. 3D and E). As shown in Fig. 3F, miR-134 overexpression upregulated E-cadherin, and downregulated α -SMA expression. In addition, western blot analysis revealed consistent alterations in the aforementioned EMT markers in the *H. pylori*_{CagA+/P+} + miR-134 mimics groups compared with in the *H. pylori*_{CagA+/P+} group (Fig. 3G). These findings indicated

that miR-134 may act as a suppressor of proliferation, invasion and EMT in *H. pylori*_{CagA+/P+}-infected SGC-7901 cells.

FoxM1 is identified as a direct target of miR-134. To determine the target gene of miR-134 in *H. pylori*_{CagA+/P+}-infected GC cells, candidate target genes were searched using bioinformatics analysis. The analysis revealed that FoxM1 possessed a putative miR-134-binding site (Fig. 4A), which prompted further validation of this relationship. FoxM1 expression was significantly increased in *H. pylori*_{CagA+/P+} GC tissues compared with in *H. pylori*_{CagA+/P-} GC tissues (Fig. 4B). Correlation analysis revealed that FoxM1 expression was negatively correlated with miR-134 expression (Fig. 4C). Subsequently, knockdown of miR-134 was achieved via transfection with miR-134 inhibitors; transfection efficiency was validated by RT-qPCR (Fig. 4D). In response to miR-134 overexpression, the mRNA and protein expression levels of FoxM1 were significantly downregulated, whereas they were upregulated by miR-134 knockdown in SGC-7901 cells (Fig. 4E and F). Dual luciferase reporter assay revealed that miR-134 mimics significantly suppressed FoxM1 wild type luciferase activity compared with in the mimics control group, but did not affect FoxM1 mutant type luciferase activity (Fig. 4G). Furthermore, immunofluorescence assay demonstrated that miR-134 mimics decreased the expression of FoxM1 protein in *H. pylori*_{CagA+/P+}-infected cells (Fig. 4H). These data suggested that FoxM1 was a direct target gene of miR-134 and was negatively regulated by miR-134.

Knockdown of FoxM1 impedes H. pylori-induced EMT. Although elevated FoxM1 is identified as a prognostic factor for GC, whether it is involved in EMT in *H. pylori*_{CagA+/P+}-associated GC remains undefined. Therefore, si-FoxM1 was used to knockdown

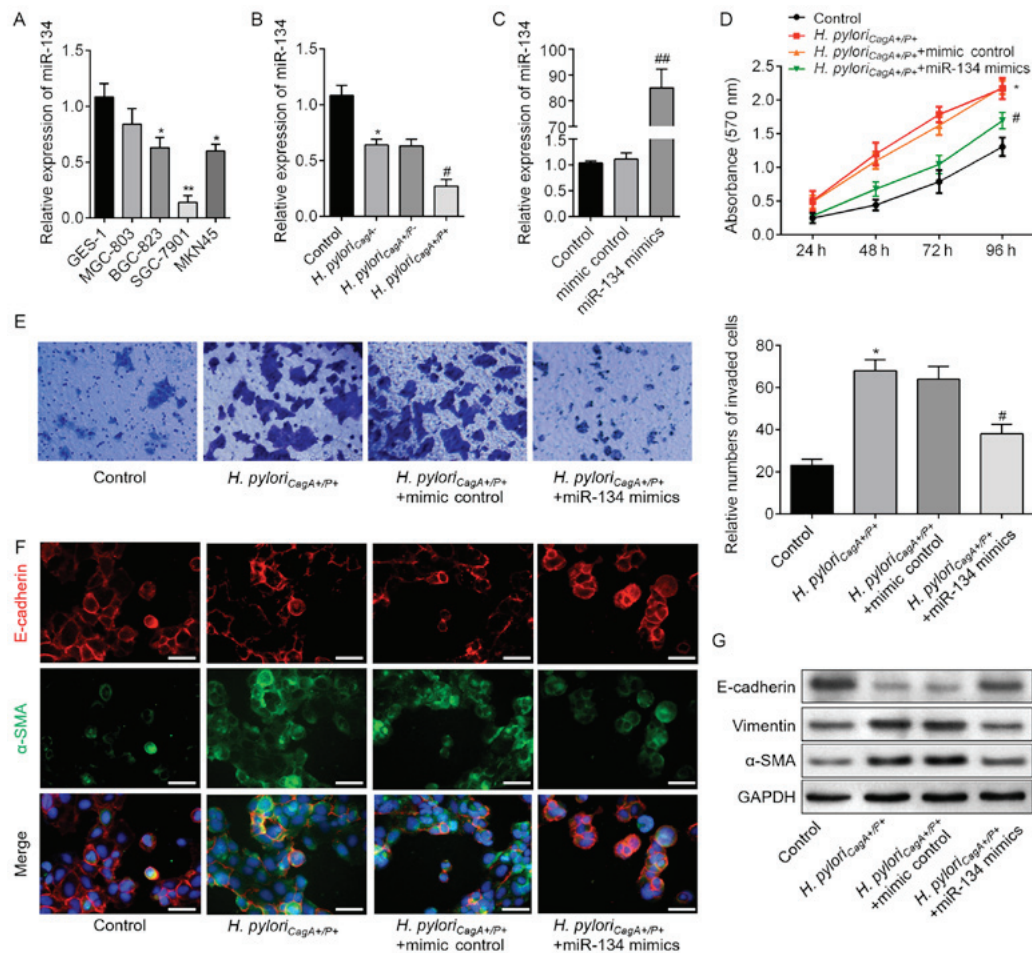


Figure 3. miR-134 inhibits proliferation, invasion and EMT in *H. pylori*_{CagA+/P+}-infected SGC-7901 cells. (A) miR-134 expression in a human gastric epithelial cell (GES-1), and MGC803, BGC-823, SGC-7901 and MKN45 gastric cancer cell lines, as detected by reverse transcription-PCR analysis. **P*<0.05, ***P*<0.01 vs. GES-1 cells. (B) Relative expression levels of miR-134 in SGC-7901 cells infected with *H. pylori*_{CagA-}, *H. pylori*_{CagA+/P-} and *H. pylori*_{CagA+/P+}. (C) Expression levels of miR-134 in SGC-7901 cells transfected with mimic control or miR-134 mimics, as evaluated by reverse transcription-qPCR assay. (D) SGC-7901 cells transfected with miR-134 mimics or mimic control under *H. pylori*_{CagA+/P+} infection were subjected to Cell Counting Kit-8 analysis. (E) Invasive SGC-7901 cells were stained with 0.1% crystal violet and counted 48 h post-transfection (magnification, x100). The number of invaded cells was determined from three replicate wells and data are expressed as the means \pm standard deviation. (F) Double-labeled immunofluorescence staining was performed to examine the expression of E-cadherin (red) and α -SMA (green) in SGC-7901 cells from the various groups. Images merged with DAPI are presented. Scale bar, 50 μ m. (G) Protein expression levels of E-cadherin, Vimentin and α -SMA in SGC-7901 cells treated as indicated. **P*<0.05 vs. the control group; #*P*<0.05 vs. the *H. pylori*_{CagA+/P+} + mimics control group. α -SMA, α -smooth muscle actin; CagA, cytotoxin-associated gene A; *H. pylori*_{CagA-}, CagA-negative *H. pylori*; *H. pylori*_{CagA+/P-}, CagA-positive and PBP1A mutation-negative *H. pylori*; *H. pylori*_{CagA+/P+}, CagA- and PBP1A mutation-positive *H. pylori*; *H. pylori*, *Helicobacter pylori*; miR-134, microRNA-134; PBP1A, penicillin-binding protein 1A; RT-qPCR, reverse transcription-quantitative polymerase chain reaction.

FoxM1 in *H. pylori*_{CagA+/P+}-infected SGC-7901 cells. The transfection efficiency of si-FoxM1 was determined using RT-qPCR and western blot analysis (Fig. 5A and B). Subsequently, the role of FoxM1 in *H. pylori*_{CagA+/P+}-induced EMT was determined. Western blot analysis revealed that *H. pylori*-mediated EMT was significantly reversed by knockdown of FoxM1 (Fig. 5C). Similarly, these findings were validated at the mRNA level, as evidenced by the alterations in EMT-associated genes (Fig. 5D-F). These data revealed that *H. pylori*_{CagA+/P+} may trigger EMT of GC cells through regulation of FoxM1.

miR-134 exerts its tumor suppressor function through regulation of FoxM1. Having demonstrated that FoxM1 is a target gene of miR-134, the present study further investigated whether it was involved in the miR-134-mediated role in *H. pylori*_{CagA+/P+}-infected GC cells. A FoxM1 plasmid was transfected into SGC-7901 cells, and the mRNA and protein expression levels of FoxM1 were significantly increased

following transfection (Fig. 6A and B). As illustrated in Fig. 6C and D, the inhibitory effects of miR-134 overexpression were reduced by co-transfection with FoxM1. Furthermore, western blotting (Fig. 6E) and RT-qPCR analysis (Fig. 6F-H) demonstrated that co-transfection with miR-134 mimics and FoxM1 markedly downregulated E-cadherin, and upregulated Vimentin and α -SMA compared with in the *H. pylori*_{CagA+/P+} + miR-134 mimics group. These data suggested that miR-134 may inhibit *H. pylori*_{CagA+/P+}-induced GC cell proliferation and invasion, and reverse EMT by regulating FoxM1 in SGC-7901 cells.

Discussion

The present study demonstrated that *H. pylori*_{CagA+/P+} was associated with poor clinicopathological characteristics in GC. In addition, *H. pylori*_{CagA+/P+} infection significantly promoted GC cell proliferation and invasion, and induced

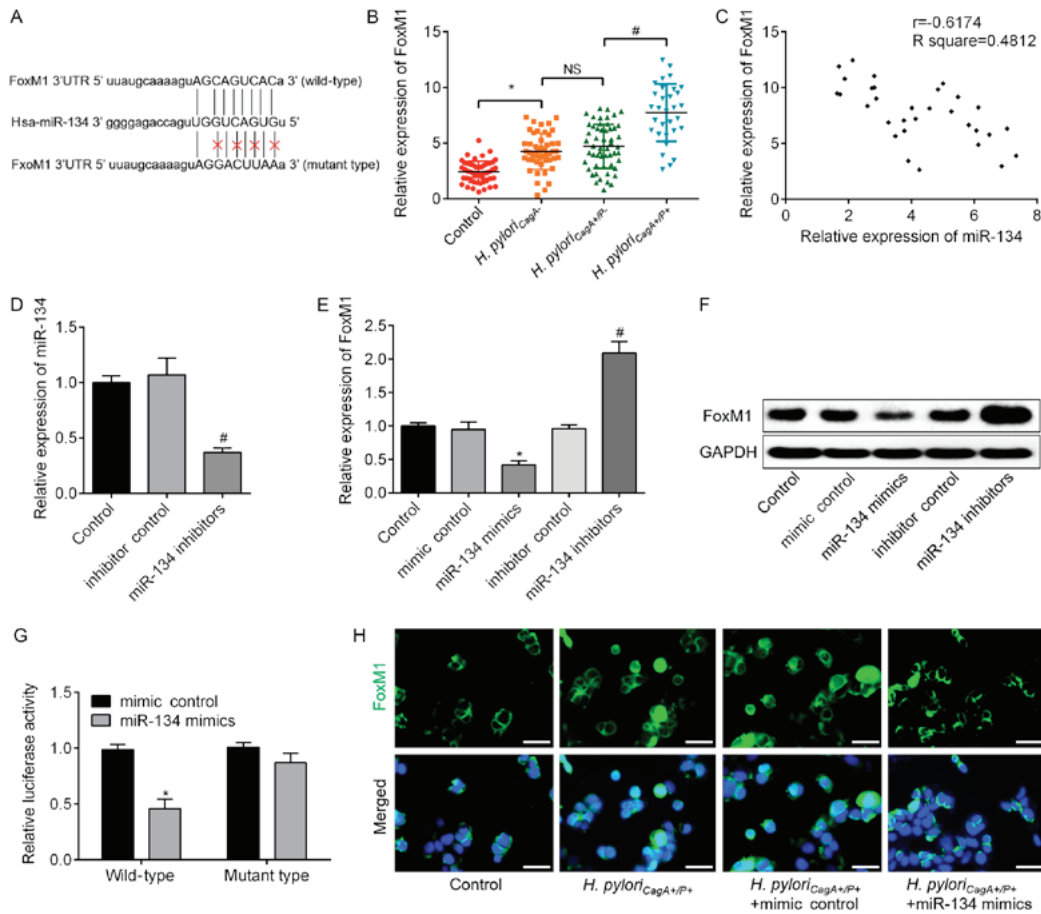


Figure 4. FoxM1 is a downstream target of miR-134, which directly binds to the 3'UTR of FoxM1. (A) Putative miR-134-binding sites in the 3'UTR of FoxM1 mRNA. A mutation was generated in the FoxM1 3'UTR sequence in the complementary site for the seed region of miR-134. (B) Relative expression levels of FoxM1 in GC tissues without *H. pylori* infection, and tissues infected with *H. pylori*_{CagA}, *H. pylori*_{CagA+/P} and *H. pylori*_{CagA+/P+}. (C) A negative correlation was observed between FoxM1 mRNA and miR-134 expression in GC tissues infected with *H. pylori*_{CagA+/P+}. (D) Expression levels of miR-134 in SGC-7901 cells transfected with inhibitor control or miR-134 inhibitors, as determined by RT-qPCR analysis. (E) mRNA expression levels of FoxM1 were analyzed by RT-qPCR analysis in SGC-7901 cells transfected with mimic control, miR-134 mimics, inhibitor control or miR-134 inhibitors. GAPDH was used as an internal control. (F) Protein expression levels of FoxM1 were determined by western blotting in the groups. GAPDH was used as an internal control. (G) Luciferase assay in 293T cells co-transfected with miR-134 mimics or mimic control and a luciferase reporter containing wild type or mutant FoxM1 3'UTR. (H) Immunofluorescence analysis revealed the alteration of FoxM1 in *H. pylori*_{CagA+/P+}-infected SGC-7901 cells transfected with miR-134 mimics or mimic control. Images merged with DAPI are presented. Scale bar, 50 μ m. *P<0.05 vs. the mimic control group; #P<0.05 vs. the inhibitor control group. 3'UTR, 3'-untranslated region; CagA, cytotoxin-associated gene A; *H. pylori*_{CagA}, CagA-negative *H. pylori*; *H. pylori*_{CagA+/P}, CagA-positive and PBP1A mutation-negative *H. pylori*; *H. pylori*_{CagA+/P+}, CagA- and PBP1A mutation-positive *H. pylori*; FoxM1, Forkhead box M1; *H. pylori*, *Helicobacter pylori*; miR-134, microRNA-134; PBP1A, penicillin-binding protein 1A; RT-qPCR, reverse transcription-quantitative polymerase chain reaction.

EMT of GC cells. The present results also demonstrated that *H. pylori*_{CagA+/P+} may promote GC cell malignant behavior through regulation of the miR-134/FoxM1 regulatory network. These data may help to further understand the role of *H. pylori*_{CagA+/P+} in gastric carcinogenesis.

Although the causal association between *H. pylori* infection and GC incidence is well established, the exact associations between *H. pylori* and the progression of GC remain largely unknown (28). The present study analyzed the association between *H. pylori* infection and the clinical characteristics of GC in GC patients without *H. pylori* infection, and in GC patients with *H. pylori*_{CagA}, *H. pylori*_{CagA+/P} and *H. pylori*_{CagA+/P+} infection. The results indicated that *H. pylori*_{CagA} infection was not significantly associated with patient characteristics. This finding was similar to the results of previous studies, which suggested that *H. pylori* infection has no association with prognosis in China, and the prognosis of *H. pylori*-negative GC is equally poor (29). However, the present study

demonstrated that patients infected with *H. pylori*_{CagA+/P} possessed a higher proportion of advanced characteristics than those with *H. pylori*_{CagA}. This result was also supported by the findings that patients with *H. pylori*_{CagA+} GC had a worse clinical outcome than those involving *H. pylori*_{CagA} strains (8). Furthermore, distinct characteristics between *H. pylori*_{CagA+/P} and *H. pylori*_{CagA+/P+} GC were observed. Therefore, the present study focused on the role of PBP1A-mutated *H. pylori* strains. In *in vitro*-selected amoxicillin-resistant *H. pylori* strains, the resistance has been suggested to result from alterations in PBP1A (30,31). A single serine-to-arginine substitution in PBP1A induces high-level amoxicillin resistance in *H. pylori* (32), which may explain the increase in naturally occurring *H. pylori* strains with a high level of amoxicillin resistance in recent years. Currently, amoxicillin remains one of the first-line antibiotics used for prophylaxis and treatment of *H. pylori*; however, the clinical significance of *H. pylori*_{CagA+/P+} in GC remains largely unknown. The present study revealed

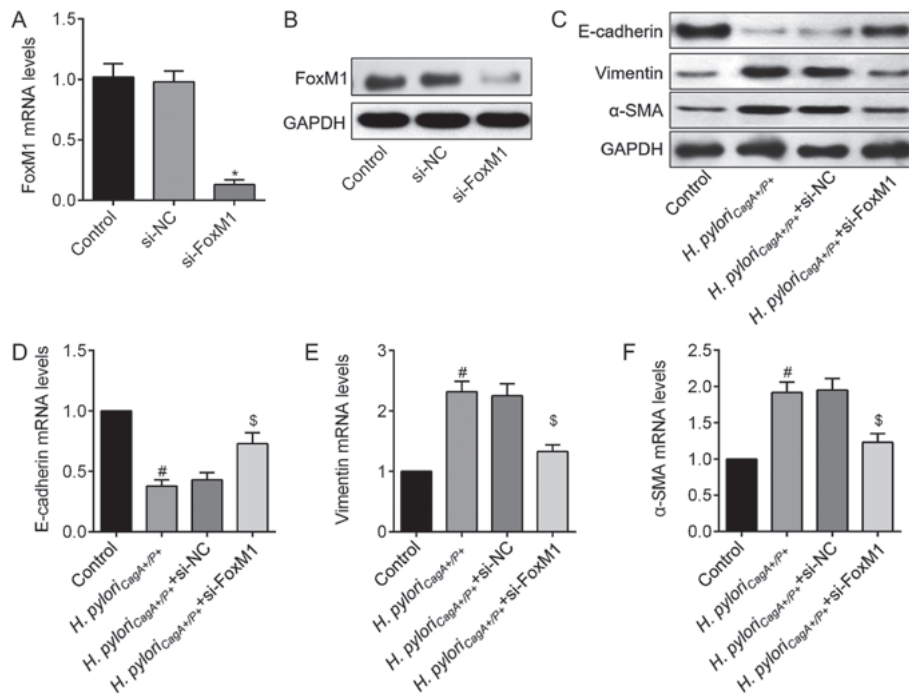


Figure 5. FoxM1 knockdown abolishes *H. pylori*_{CagA+/P+}-induced EMT in SGC-7901 cells. (A) FoxM1 mRNA expression levels in cells transfected with si-NC or si-FoxM1. (B) FoxM1 protein expression was detected following transfection with si-NC or si-FoxM1. (C) Protein expression levels of EMT markers, E-cadherin, Vimentin and α -SMA, in SGC-7901 cells transfected with si-NC or si-FoxM1, and infected with *H. pylori*_{CagA+/P+}. Relative mRNA expression levels of (D) E-cadherin, (E) Vimentin and (F) α -SMA in SGC-7901 cells, as determined by reverse transcription-quantitative polymerase chain reaction analysis. * $P < 0.05$ vs. the si-NC group; # $P < 0.05$ vs. the control group; \$ $P < 0.05$ vs. the *H. pylori*_{CagA+/P+} group. α -SMA, α -smooth muscle actin; CagA, cytotoxin-associated gene A; EMT, epithelial-mesenchymal transition; *H. pylori*_{CagA-}, CagA-negative *H. pylori*; *H. pylori*_{CagA+/P-}, CagA-positive and PBP1A mutation-negative *H. pylori*; *H. pylori*_{CagA+/P+}, CagA- and PBP1A mutation-positive *H. pylori*; FoxM1, Forkhead box M1; *H. pylori*, *Helicobacter pylori*; NC, negative control; si, small interfering RNA.

that *H. pylori*_{CagA+/P+} infection was significantly associated with various clinicopathological parameters, including invasion depth, lymphatic metastasis and distant metastasis. However, due to problems with follow-up, the 5 year overall or disease-free survival rates among the different *H. pylori* strain-infected cohorts were not analyzed. The present study hypothesized that *H. pylori*_{CagA+/P+} infection may be associated with a poorer outcome for patients with GC as compared to those with *H. pylori*_{CagA+/P-} infection.

The present study further investigated the mechanisms underlying the clinical significance of *H. pylori*_{CagA+/P+} infection. EMT is a well-characterized embryological process that serves a critical role in tumor metastasis. EMT is characterized by the loss of epithelial markers (e.g., E-cadherin) and the acquisition of mesenchymal markers (e.g., Vimentin and α -SMA) (33). The present results revealed that *H. pylori*_{CagA+/P+} induced a significant increase in cell proliferation and invasion, a decrease in E-cadherin expression, and an increase in Vimentin and α -SMA expression. Furthermore, since emerging evidence has suggested that miRNAs serve an important role in the control of *H. pylori* infection-associated responses in GC (34), this study investigated whether miRNAs were involved in *H. pylori*_{CagA+/P+}-induced EMT in GC. To determine the miRNA expression profiles in *H. pylori*_{CagA+/P+}-associated GC, a microarray chip was used to measure miRNA expression levels in GC tissues with *H. pylori*_{CagA+/P+} or *H. pylori*_{CagA+/P-} infection. Notably, miR-134 was specifically downregulated in *H. pylori*_{CagA+/P+}-infected tissues compared with those with *H. pylori*_{CagA+/P-} infection.

Aberrant levels of miR-134 have been detected in various malignancies, and may regulate tumor development, differentiation, proliferation, invasion and metastasis (35,36). Overexpression of miR-134 inhibits migration, invasion and EMT of lung cancer cells by targeting integrin $\beta 1$ mRNA (37). Similarly, Zha *et al* revealed that miR-134 specifically targets integrin $\beta 1$ to suppress the invasion and metastasis of hepatocellular carcinoma cells *in vitro* and *in vivo* (38). Additionally, forced expression of miR-134 inhibits the migration and invasion of renal cell carcinoma cells by blocking EMT (39). These findings indicated the miR-134 may serve as a tumor suppressor in human cancer (40); however, the pathogenetic roles of miR-134 were obscure in GC, particularly in GC associated with *H. pylori* infection. To the best of our knowledge, the current study was the first to reveal that forced overexpression of miR-134 could significantly reverse *H. pylori*_{CagA+/P+} infection-induced cell proliferation, invasion and EMT. Notably, the molecular and modulated mechanisms of miRNA are complex and variable (41), and a recent study revealed that miR-134 has diverse target genes in cancer (40). Using bioinformatics analysis and molecular experiments, the present study demonstrated that the downregulation of miR-134 in *H. pylori*_{CagA+/P+}-infected GC tissues was associated with upregulated FoxM1 mRNA and protein expression. In agreement with the sequence alignment, the luciferase reporter assays confirmed the direct targeting of the FoxM1 3'-untranslated region by miR-134, and suggested that a strong affinity may exist between miR-134 and FoxM1 mRNA in patients with GC and *H. pylori*_{CagA+/P+} infection.

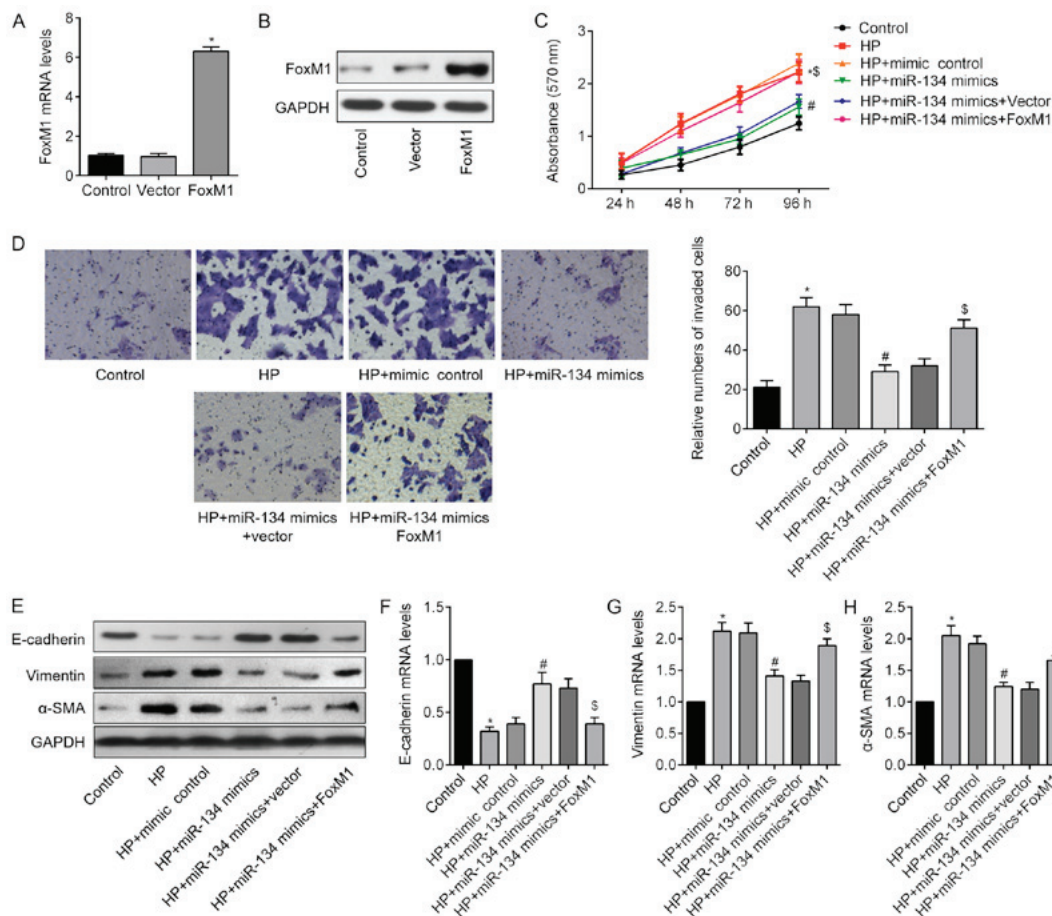


Figure 6. FoxM1 overexpression reverses miR-134-mediated HP-induced EMT in SGC-7901 cells. (A) Alteration of FoxM1 mRNA expression in groups transfected with a control vector or FoxM1 plasmid. (B) FoxM1 protein expression following transfection with a FoxM1 plasmid. (C) Cell proliferation was assessed in HP-infected SGC-7901 cells co-transfected with miR-134 mimics and FoxM1-expressing plasmid or empty vector. * $P < 0.05$ HP + mimic control vs. control group; # $P < 0.05$ HP + miR-134 mimics vs. HP + mimic control group; \$ $P < 0.05$ HP + miR-134 mimics + FoxM1 vs. HP + miR-134 mimics + Vector group. (D) Transwell assays were used to determine the invasive properties of SGC-7901 cells following various interventions; the number of invasive cells in the groups was compared (magnification, x100). (E) Western blotting was used to determine alterations in the protein expression levels of EMT markers in GC cells following various treatments. Relative mRNA expression levels of (F) E-cadherin, (G) Vimentin and (H) α -SMA in SGC-7901 cells. * $P < 0.05$ vs. the control group; # $P < 0.05$ vs. the HP group; \$ $P < 0.05$ vs. the HP + miR-134 mimics group. α -SMA, α -smooth muscle actin; CagA, cytotoxin-associated gene A; EMT, epithelial-mesenchymal transition; HP, CagA- and PBP1A mutation-positive *Helicobacter pylori*; FoxM1, Forkhead box M1; miR-134, microRNA-134.

FoxM1 shares homology with the winged helix DNA-binding domain and is predominantly expressed in fetal tissue. It is maintained ubiquitously in all proliferating adult tissues and some cancer cell lines, whereas its expression is absent from differentiated cells (42). The role of FoxM1 in the progression of GC has previously been investigated. Promotion of gastric tumorigenesis by FoxM1 is directly and significantly correlated with transactivation of vascular endothelial growth factor expression and elevation of angiogenesis (43). Increased FOXM1 expression is also associated with invasive and metastatic processes in GC, and is inversely associated with patient prognosis (44). Mechanistically, FOXM1 promotes GC cell migration and invasion through inducing the expression of Cath-D (45). Furthermore, a negative correlation has been identified between FoxM1 and E-cadherin expression in GC tissue (46). E-cadherin is associated with epithelial phenotypes, which serve a critical role in the process of EMT (47). In accordance with the previous study, the present results indicated that knockdown of FoxM1 significantly abolished *H. pylori*-induced EMT of SGC-7901 cells. The functional studies revealed that the effects of miR-134 on cell

proliferation, invasion and EMT were reversed by FoxM1 overexpression. Although a previous study revealed that FoxM1 is overexpressed in *H. pylori*_{CagA+}-induced gastric carcinogenesis and is regulated by miR-370 (48), the present study is the first, to the best of our knowledge, to suggest that FoxM1 was involved in *H. pylori*_{CagA+/P+}-mediated GC cell EMT and was negatively controlled by miR-134, delineating the mechanisms governing FoxM1 regulation in GC.

The present study has numerous limitations. The number of clinical samples used in this study was relatively small and further studies are required to validate the role of *H. pylori*_{CagA+/P+} infection in patients with GC. Additionally, *H. pylori* infections in many patients are asymptomatic and only a few people develop clinical disease (49). However, focusing on the pathways implicated in *H. pylori*-induced tumorigenesis may lead to novel therapeutic strategies for GC prevention. In addition, with the growing proportion of amoxicillin-resistant *H. pylori*, a kit for detection of PBP1A mutations would be beneficial in clinical practice.

In conclusion, the present study revealed that *H. pylori*_{CagA+/P+} was associated with poor clinicopathological characteristics

in patients with GC. In addition, *H. pylori*_{CagA+/P+} induced significant cell proliferation, invasion and EMT of GC cells. Mechanistically, *H. pylori*_{CagA+/P+} promoted EMT of GC cells through suppressing miR-134, which targeted FoxM1 in GC.

Acknowledgements

Not applicable.

Funding

The study was supported by Natural Science Funding of China (grant nos. 31671869, 31471598, 31571852 and 31601487).

Availability of data and materials

All data generated or analyzed during this study are included in this published article.

Authors' contributions

DDP designed the study and performed the statistical analysis; LH and ZYW performed the experiments and data correction; LH wrote the manuscript.

Ethics approval and consent to participate

The present study was approved by the ethical board of the Jiangsu Province Hospital of TCM (ethical no. JSSZY2014085). All studies performed involving human participants were conducted in accordance with the Strengthening the Reporting of Observational Studies in Epidemiology guidelines, and the 2013 Declaration of Helsinki. The patients, or their parents, provided written informed consent.

Patient consent for publication

Not applicable.

Competing interests

The authors declare that they have no competing interests.

References

1. Ferlay J, Soerjomataram I, Dikshit R, Eser S, Mathers C, Rebelo M, Parkin DM, Forman D and Bray F: Cancer incidence and mortality worldwide: Sources, methods and major patterns in GLOBOCAN 2012. *Int J Cancer* 136: E359-E386, 2015.
2. Choi JI, Kook MC, Kim YI, Cho SJ, Lee JY, Kim CG, Park B and Nam BH: *Helicobacter pylori* Therapy for the Prevention of Metachronous Gastric Cancer. *N Engl J Med* 378: 1085-1095, 2018.
3. Greenberg ER, Anderson GL, Morgan DR, Torres J, Chey WD, Bravo LE, Dominguez RL, Ferreccio C, Herrero R, Lazcano-Ponce EC, *et al*: 14-day triple, 5-day concomitant, and 10-day sequential therapies for *Helicobacter pylori* infection in seven Latin American sites: A randomised trial. *Lancet* 378: 507-514, 2011.
4. Lee YC, Chiang TH, Chou CK, Tu YK, Liao WC, Wu MS and Graham DY: Association Between *Helicobacter pylori* Eradication and Gastric Cancer Incidence: A Systematic Review and Meta-analysis. *Gastroenterology* 150: 1113-1124.e5, 2016.
5. Wang F, Sun GP, Zou YF, Zhong F, Ma T, Li XQ and Wu D: *Helicobacter pylori* infection predicts favorable outcome in patients with gastric cancer. *Curr Oncol* 20: e388-e395, 2013.
6. Wang F, Sun G, Zou Y, Zhong F, Ma T and Li X: Protective role of *Helicobacter pylori* infection in prognosis of gastric cancer: Evidence from 2,454 patients with gastric cancer. *PLoS One* 8: e62440, 2013.
7. Zheng F, Sun Z, Kan J, Yin J, Du F, Shen G, Wang Z, Ren D, Bao X and Zhao J: Is It a Protective Factor of *Helicobacter pylori* Infection in Overall Survival of All Gastric Cancer? Evidence from Meta-Analysis. *J Environ Pathol Toxicol Oncol* 36: 309-320, 2017.
8. Varga MG, Wang T, Cai H, Xiang YB, Gao YT, Ji BT, Pawlita M, Waterboer T, Zheng W, Shu XO, *et al*: *Helicobacter pylori* Blood Biomarkers and Gastric Cancer Survival in China. *Cancer Epidemiol Biomarkers Prev* 27: 342-344, 2018.
9. Malfertheiner P, Megraud F, O'Morain CA, Atherton J, Axon AT, Bazzoli F, Gensini GF, Gisbert JP, Graham DY, Rokkas T, *et al*: European *Helicobacter* Study Group: Management of *Helicobacter pylori* infection - the Maastricht IV/Florence Consensus Report. *Gut* 61: 646-664, 2012.
10. Morgan DR, Torres J, Sexton R, Herrero R, Salazar-Martínez E, Greenberg ER, Bravo LE, Dominguez RL, Ferreccio C, Lazcano-Ponce EC, *et al*: Risk of recurrent *Helicobacter pylori* infection 1 year after initial eradication therapy in 7 Latin American communities. *JAMA* 309: 578-586, 2013.
11. Nagai K, Davies TA, Jacobs MR and Appelbaum PC: Effects of amino acid alterations in penicillin-binding proteins (PBPs) 1a, 2b, and 2x on PBP affinities of penicillin, ampicillin, amoxicillin, cefditoren, cefuroxime, cefprozil, and cefaclor in 18 clinical isolates of penicillin-susceptible, -intermediate, and -resistant pneumococci. *Antimicrob Agents Chemother* 46: 1273-1280, 2002.
12. Polk DB and Peek RM Jr: *Helicobacter pylori*: Gastric cancer and beyond. *Nat Rev Cancer* 10: 403-414, 2010.
13. Park JY, Forman D, Waskito LA, Yamaoka Y and Crabtree JE: Epidemiology of *Helicobacter pylori* and CagA-Positive Infections and Global Variations in Gastric Cancer. *Toxins (Basel)* 10: 10, 2018.
14. Yong X, Tang B, Li BS, Xie R, Hu CJ, Luo G, Qin Y, Dong H and Yang SM: *Helicobacter pylori* virulence factor CagA promotes tumorigenesis of gastric cancer via multiple signaling pathways. *Cell Commun Signal* 13: 30, 2015.
15. Sokolova O, Borgmann M, Rieke C, Schweitzer K, Rothkötter HJ and Naumann M: *Helicobacter pylori* induces type 4 secretion system-dependent, but CagA-independent activation of IκBs and NF-κB/RelA at early time points. *Int J Med Microbiol* 303: 548-552, 2013.
16. Yoon JH, Seo HS, Choi SS, Chae HS, Choi WS, Kim O, Ashktorab H, Smoot DT, Nam SW, Lee JY, *et al*: Gastrokine 1 inhibits the carcinogenic potentials of *Helicobacter pylori* CagA. *Carcinogenesis* 35: 2619-2629, 2014.
17. Cadamuro AC, Rossi AF, Maniezzo NM and Silva AE: *Helicobacter pylori* infection: Host immune response, implications on gene expression and microRNAs. *World J Gastroenterol* 20: 1424-1437, 2014.
18. Verma R and Sharma PC: Next generation sequencing-based emerging trends in molecular biology of gastric cancer. *Am J Cancer Res* 8: 207-225, 2018.
19. Ueda T, Volinia S, Okumura H, Shimizu M, Taccioli C, Rossi S, Alder H, Liu CG, Oue N, Yasui W, *et al*: Relation between microRNA expression and progression and prognosis of gastric cancer: A microRNA expression analysis. *Lancet Oncol* 11: 136-146, 2010.
20. Siu LK, Leung WK, Cheng AF, Sung JY, Ling TK, Ling JM, Ng EK, Lau JY and Chung SC: Evaluation of a selective transport medium for gastric biopsy specimens to be cultured for *Helicobacter pylori*. *J Clin Microbiol* 36: 3048-3050, 1998.
21. Atrisco-Morales J, Martínez-Santos VI, Román-Román A, Alarcón-Millán J, De Sampedro-Reyes J, Cruz-Del Carmen I, Martínez-Carrillo DN and Fernández-Tilapa G: vacA s1m1 genotype and cagA EPIYA-ABC pattern are predominant among *Helicobacter pylori* strains isolated from Mexican patients with chronic gastritis. *J Med Microbiol* 67: 314-324, 2018.
22. Kwon YH, Kim JY, Kim N, Park JH, Nam RH, Lee SM, Kim JW, Kim JM, Park JY and Lee DH: Specific mutations of penicillin-binding protein 1A in 77 clinically acquired amoxicillin-resistant *Helicobacter pylori* strains in comparison with 77 amoxicillin-susceptible strains. *Helicobacter* 22: 22, 2017.
23. Bisignano C, Filocamo A, La Camera E, Zummo S, Fera MT and Mandalari G: Antibacterial activities of almond skins on cagA-positive and-negative clinical isolates of *Helicobacter pylori*. *BMC Microbiol* 13: 103, 2013.

24. Qureshi NN, Gallaher B and Schiller NL: Evolution of amoxicillin resistance of *Helicobacter pylori* in vitro: Characterization of resistance mechanisms. *Microb Drug Resist* 20: 509-516, 2014.
25. Al-Maleki AR, Loke MF, Lui SY, Ramli NSK, Khosravi Y, Ng CG, Venkatraman G, Goh KL, Ho B and Vadivelu J: *Helicobacter pylori* outer inflammatory protein A (OipA) suppresses apoptosis of AGS gastric cells in vitro. *Cell Microbiol* 19: 19, 2017.
26. Yang J, Song H, Cao K, Song J and Zhou J: Comprehensive analysis of *Helicobacter pylori* infection-associated diseases based on miRNA-mRNA interaction network. *Brief Bioinform*: Mar 20, 2018 (Epub ahead of print).
27. Livak KJ and Schmittgen TD: Analysis of relative gene expression data using real-time quantitative PCR and the 2⁻(Delta Delta C(T)) method. *Methods* 25: 402-408, 2001.
28. Yang Y, Li X, Du J, Yin Y and Li Y: Involvement of microRNAs-MMPs-E-cadherin in the migration and invasion of gastric cancer cells infected with *Helicobacter pylori*. *Exp Cell Res* 367: 196-204, 2018.
29. Tsai KF, Liou JM, Chen MJ, Chen CC, Kuo SH, Lai IR, Yeh KH, Lin MT, Wang HP, Cheng AL, *et al*; Taiwan Gastrointestinal Disease and Helicobacter Consortium: Distinct Clinicopathological Features and Prognosis of *Helicobacter pylori* Negative Gastric Cancer. *PLoS One* 12: e0170942, 2017.
30. DeLoney CR and Schiller NL: Characterization of an In vitro-selected amoxicillin-resistant strain of *Helicobacter pylori*. *Antimicrob Agents Chemother* 44: 3368-3373, 2000.
31. Paul R, Postius S, Melchers K and Schäfer KP: Mutations of the *Helicobacter pylori* genes *rdxA* and *pbpI* cause resistance against metronidazole and amoxicillin. *Antimicrob Agents Chemother* 45: 962-965, 2001.
32. Gerrits MM, Schuijffel D, van Zwet AA, Kuipers EJ, Vandenbroucke-Grauls CM and Kusters JG: Alterations in penicillin-binding protein 1A confer resistance to beta-lactam antibiotics in *Helicobacter pylori*. *Antimicrob Agents Chemother* 46: 2229-2233, 2002.
33. Liang L, Zeng M, Pan H, Liu H and He Y: Nicotinamide N-methyltransferase promotes epithelial-mesenchymal transition in gastric cancer cells by activating transforming growth factor- β 1 expression. *Oncol Lett* 15: 4592-4598, 2018.
34. Polakovicova I, Jerez S, Wichmann IA, Sandoval-Bórquez A, Carrasco-Véliz N and Corvalán AH: Role of microRNAs and Exosomes in *Helicobacter pylori* and Epstein-Barr Virus Associated Gastric Cancers. *Front Microbiol* 9: 636, 2018.
35. Li J, Wang Y, Luo J, Fu Z, Ying J, Yu Y and Yu W: miR-134 inhibits epithelial to mesenchymal transition by targeting FOXM1 in non-small cell lung cancer cells. *FEBS Lett* 586: 3761-3765, 2012.
36. Liu CJ, Shen WG, Peng SY, Cheng HW, Kao SY, Lin SC and Chang KW: miR-134 induces oncogenicity and metastasis in head and neck carcinoma through targeting WWOX gene. *Int J Cancer* 134: 811-821, 2014.
37. Qin Q, Wei F, Zhang J and Li B: miR-134 suppresses the migration and invasion of non small cell lung cancer by targeting ITGB1. *Oncol Rep* 37: 823-830, 2017.
38. Zha R, Guo W, Zhang Z, Qiu Z, Wang Q, Ding J, Huang S, Chen T, Gu J, Yao M, *et al*: Genome-wide screening identified that miR-134 acts as a metastasis suppressor by targeting integrin β 1 in hepatocellular carcinoma. *PLoS One* 9: e87665, 2014.
39. Liu Y, Zhang M, Qian J, Bao M, Meng X, Zhang S, Zhang L, Zhao R, Li S, Cao Q, *et al*: miR-134 functions as a tumor suppressor in cell proliferation and epithelial-to-mesenchymal Transition by targeting KRAS in renal cell carcinoma cells. *DNA Cell Biol* 34: 429-436, 2015.
40. Pan JY, Zhang F, Sun CC, Li SJ, Li G, Gong FY, Bo T, He J, Hua RX, Hu WD, *et al*: miR-134: A Human Cancer Suppressor? *Mol Ther Nucleic Acids* 6: 140-149, 2017.
41. Bartel DP: MicroRNAs: Target recognition and regulatory functions. *Cell* 136: 215-233, 2009.
42. Korver W, Roose J and Clevers H: The winged-helix transcription factor Trident is expressed in cycling cells. *Nucleic Acids Res* 25: 1715-1719, 1997.
43. Li Q, Zhang N, Jia Z, Le X, Dai B, Wei D, Huang S, Tan D and Xie K: Critical role and regulation of transcription factor FoxM1 in human gastric cancer angiogenesis and progression. *Cancer Res* 69: 3501-3509, 2009.
44. Ma J, Qi G, Xu J, Ni H, Xu W, Ru G, Zhao Z, Xu W and He X: Overexpression of forkhead box M1 and urokinase-type plasminogen activator in gastric cancer is associated with cancer progression and poor prognosis. *Oncol Lett* 14: 7288-7296, 2017.
45. Yang L, Cui M, Zhang L and Song L: FOXM1 facilitates gastric cancer cell migration and invasion by inducing Cathepsin D. *Oncotarget* 8: 68180-68190, 2017.
46. Zhang J, Chen XY, Huang KJ, Wu WD, Jiang T, Cao J, Zhou LS, Qiu ZJ and Huang C: Expression of FoxM1 and the EMT-associated protein E-cadherin in gastric cancer and its clinical significance. *Oncol Lett* 12: 2445-2450, 2016.
47. Yu H, Shen Y, Hong J, Xia Q, Zhou F and Liu X: The contribution of TGF- β in Epithelial-Mesenchymal Transition (EMT): Down-regulation of E-cadherin via snail. *Neoplasma* 62: 1-15, 2015.
48. Feng Y, Wang L, Zeng J, Shen L, Liang X, Yu H, Liu S, Liu Z, Sun Y, Li W, *et al*: FoxM1 is overexpressed in *Helicobacter pylori*-induced gastric carcinogenesis and is negatively regulated by miR-370. *Mol Cancer Res* 11: 834-844, 2013.
49. Gunawardhana N, Jang S, Choi YH, Hong YA, Jeon YE, Kim A, Su H, Kim JH, Yoo YJ, Merrell DS, *et al*: *Helicobacter pylori*-Induced HB-EGF Upregulates Gastrin Expression via the EGF Receptor, C-Raf, Mek1, and Erk2 in the MAPK Pathway. *Front Cell Infect Microbiol* 7: 541, 2018.



This work is licensed under a Creative Commons Attribution-NonCommercial-NoDerivatives 4.0 International (CC BY-NC-ND 4.0) License.